International Scientific Colloquium
Modelling for Material Processing
Riga, June 8-9, 2006

Investigation of Transient Flow Behaviour in Dual-scale Porous Media with Micro Particle Image Velocimetry

M. Nordlund, T.S. Lundström

Abstract

Injection processing of composite materials most often includes infiltration of a thermoset resin into a multi-scale porous fabric. Controlling the fluid flow within the multi-scale fabric is essential for the quality of the final composite material, since the transport of fluid between regions with different scales plays an important role in phenomena such as void formation and filtration of particle doped resins.

In this work, the transient flow behaviour in dual scale porous media is investigated with Micro Particle Image Velocimetry in order to enhance the knowledge and control of the processing of multi-scale composites so that their quality can be improved. Experiments show that the fluid transport between the two scales can be controlled by the injection velocity. Validation of the measured velocity fields furthermore shows excellent agreement with theory.

Introduction

Manufacturing of fibre reinforced composite materials always includes an impregnation stage, where resin is allowed to flow into a geometry. During impregnation, air/fibre interfaces are replaced by resin/fibre interfaces at the flow front. A pressure difference is present over the flow front due to the difference in surface tension between the resin and the air. This pressure difference, called capillary pressure drop can either enhance or work against the filling depending on the curvature of the interface surface [1]. A multi-scale geometry, built from fibre bundles, results in an inhomogeneous wetting of the fabric. This implies that there will be non-uniform flow front propagation in the fabric, since the flow can be leading either in the micro-scale fibre bundles or in the meso-scale inter-bundle channels depending on the dynamic wetting behaviour of the fluid in combination with the injection velocity [2]. In [3-6] it is shown that these effects play important roles in void formation during low pressure injections. An optimal resin infiltration velocity was found in [4; 5] which reduces void formation. The optimal state implies that neither the micro-scale flow in the fibre bundles nor the meso-scale flow in the inter-bundle spacings is leading. Below this value, where the capillary effects are dominant over the viscous effects, the flow is leading in the fibre bundles and can entrap voids in the meso-scale regions and the other way around when the flow is leading in the meso-scale regions. The lack of capillary effects in saturated flow conditions results in that the flow in the meso-scale geometry is dominating over the micro-scale flow [7].

Micro Particle Image Velocimetry (μPIV) is a measurement technique to determine velocity fields in micro-scale geometries. This was exemplified for flows through porous media in [8; 9], where the measured two-dimensional flows through hexagonal arrangement of cylindrical rods showed good agreement with existing theory. The problem of multi-scale

porosity was furthermore studied in [8; 10; 11], where the flow in the transition zone between the porous medium and the meso-scale geometry were investigated. In [12], reflective index matched μPIV showed that the transition layer between the two different porosities is of the order of the fibre diameter of the porous media instead of $\sqrt{K}$, where K is the permeability, as predicted by the theory for steady state flow conditions. The result is furthermore supported by investigations presented in [10; 11]. Complex multi-scale geometries rather that structured porous media were studied in [13] in order to develop and validate a theoretical model describing the dual-scale flow and in [14] to investigate the systematic error produced by the interrogation volumes in the μPIV method, respectively.

Transient micro-scale flow has been studied in [15], where refractive index matched μPIV was used to measure the velocity field in the vicinity of a meniscus in a capillary tube. It was shown that symmetrical vorticies are produced behind the meniscus. Furthermore, a measurement technique in order to study fast transient flow phenomena was developed using high speed μPIV measurements in [16].

As discussed above, experimental investigations of the steady state flow conditions in the interface region of multi-scale porosities has been presented, but there is still a lack of understanding of the transient velocity field and the mass transfer between regions of different scales in the vicinity of a flow front in multi-scale porous media. This flow phenomenon, together with its implication to the processing stage of composite manufacturing, is therefore studied in detail in the present work by the use of μPIV measurements.

1. Theory

Steady state flow through a multi scale porous media, consisting of micro-scale and meso-scale regions, experiences different flow conditions in different regions. In the micro-scale region, the flow can often be described using Brinkman equation [17]:

$$\nabla p = -\frac{\mu}{K}u + \mu\nabla^2 u \ , \tag{1.1}$$

where p is the pressure, u the velocity vector, μ the viscosity and K the permeability, whereas the meso-scale flow in the channel can be approximated by Stokes equation when inertia is negligible [18]

$$\nabla p = \mu\nabla^2 u \ . \tag{1.2}$$

In thin, rectangular channels, the permeability can be calculated analytically by assuming Stokes flow between two indefinitely large, parallel plates to be $h_s^2/12$, where h_s is the distance between the plates. Matching Eqn:s (1.1) and (1.2), with boundary conditions preserving continuity, results in an expression for the theoretical velocity profile, which will be used to validate the experiments.

μPIV is a technique for measuring velocity fields in microscopic fluid systems. The technique is based on cross-correlation of double framed images with a short time difference dt, of illuminated, fluorescent tracer particles in the flow field. A double pulsed laser source, synchronized with a double framed CCD camera, is used for the recording of time series of double framed images. Since the entire fluid domain is illuminated in μPIV, the measurement plane is set by the focal plane of the microscope.

The velocity field is calculated by a cross-correlation algorithm based on Fast Fourier Transform (FFT), which calculates the particle displacements between the two frames in small

interrogation areas and transforms them to velocity vectors. A multi-pass algorithm using two passes with interrogation areas of 128×128 pixels with 50% overlap and 1 pass with 64×64 pixels area and 75% overlap is used in order to improve the correlation where the tracer particle density is low.

In order to perform successful correlation between two images, the displacements of tracer particles have to be sufficiently large, to give a strong cross-correlation peak, but small enough to keep the particles in the same interrogation areas [19]. The different flow rates occurring in multi-scale geometries create problems when performing cross-correlation in the entire flow domain. While certain regions result in satisfactory correlation, other regions suffer from insufficient particle displacements. In these situations, partitioning of the fluid domain can enhance the results. The velocity field in regions with too low particle displacement can be calculated by cross-correlating subsequent images in the time-series of double framed images, instead of the double framed images themselves. The *dt*:s between subsequent, double framed images are determined by the acquisition frequency and is hence larger than the *dt* between the two images in the double frame. This results in sufficient particle displacement even in the regions with low fluid velocity.

In steady state flow conditions, a summation of correlation functions from several image pairs in a time-series can be carried out, in order to provide a reliably, time-averaged velocity field. The accuracy of the correlations is greatly improved over the entire flow field with this technique compared to calculation of average velocity fields from single cross-correlations [20].

2. Experimental setup and measurement techniques

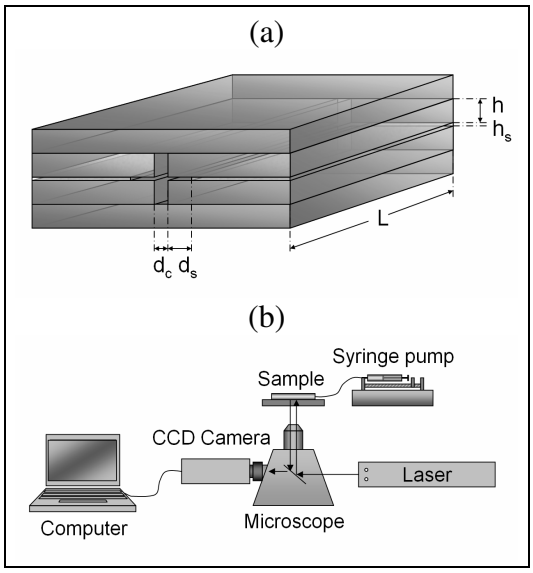

Fig. 1. (a) Multi-scale channel model (b) μPIV system.

The experimental setup consists of a closed dual-scale, rectangular horizontal channel made from glass with dimensions: h=1.00 mm, h_s=0.136 mm, d_c=0.72 mm, d_s=0.50 and L = 40 mm, cf. Fig. 1. The channel consists of a meso-scale, rectangular channel and two thin, rectangular slits at each side of the channel, cf. Fig. 1. The slit regions have widths d_s and thickness h_s and are build up between double sided adhesive tapes separated with a distance of $d_c + 2 \cdot d_s$. The fluid used in the present experiments is a 88 percentage glycerol/water mixture. The viscosity for the mixture at the temperature 22°C is 0.133 Pas [21]. The tracer particles used are fluorescent MF-RhB-2150 particles with diameters of 10.20 μm ± 0.17 μm from MicroParticles Gmbh. The flow was driven with a constant flow rate controlled by a KdScientific 100-series syringe pump with a 60 ml syringe.

The μ-PIV system consists of a 100 Hz double pulsed Nd-YAG laser with a wavelength of 532 nm from Litron and a LaVision FlowMaster Imager Pro camera (> 300 Hz) with a spatial resolution of 1280×1024 pixels mounted to a Zeiss Axiovert 200 microscope with a Zeiss EC Plan-NEOFLUAR 10x/0.3 lens, cf. Fig. 1(b).

Tab. 1. Experimental data

Experiments (Set)	Q [m^3s^{-1}]	Re
Exp1-3 (1)	$4.2 \cdot 10^{-8}$	$2.2 \cdot 10^{-4}$
Exp4-6 (2)	$1.4 \cdot 10^{-8}$	$7.4 \cdot 10^{-5}$
Exp7-9 (3)	$2.8 \cdot 10^{-9}$	$1.5 \cdot 10^{-5}$

Three sets of experiments with three experiments in each set have been performed for different flow rates, Q, in order to investigate the transient velocity field in the vicinity of the flow front and its dependence on the injection velocity, cf. Tab. 1. Double framed images are recorded at a distance of 17.0 mm from the inlet of the dual-scale channel with a frequency of 20 Hz and time step, dt = 1562 μs between the frames. The acquisition time for the experiments in Set 1 and 2 was 3 seconds, while it was 6 seconds for the lower Q in Set 3. The flow fronts are determined by image analysis from the recorded images.

3. Results and Discussion

The flow fronts for the experiments indicate that for the experiments in Set 1, the flow is clearly leading in the meso-scale channel flow and lagging in the slit region, cf. Fig. 2. The results also indicates that the shape of the flow front in the meso-scale channel is convex for the flow condition in Set 1 and 2, while it is concave in Set 3, where the flow front propagation is slightly leading in the slit region. The dynamic wetting behaviour is therefore changing from non-wetting to wetting behaviour as the flow rate is decreased. This result implies that the flow front behaviour can be controlled by the injection velocity in multi-scale geometries in order to give specific, transient flow behaviour. Controlling the flow to neither lead in the meso-scale channel region nor in the slit region may lead to a significant reduction in voids in composite processing as was found in [3-6].

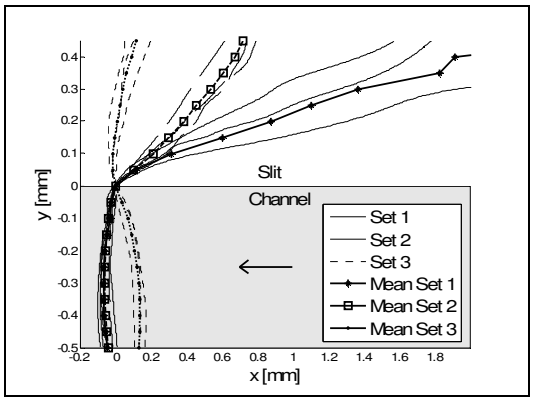

Fig. 2. Flow fronts for the three sets of experiments.

The velocity field in the vicinity of the flow front shows a similar behaviour in the meso-scale channel as in [15], where fluid in the centre of the channel is transported outwards towards the edges of the channel, see Fig. 3(a), (b). There are also relatively large transversal velocity components in the slit region, transferring fluid into the slit from the meso-scale region by capillary forces. An interesting phenomenon is observed in Fig. 3(a) representing Set 1, where the transversal velocity is acting over a relatively large distance from the flow front, whereas it is only present in the close vicinity of the front for the flow condition in Set 3, cf. Fig. 3(b). The directions of the velocity vectors in neighbourhood of the front in the slit region are furthermore steeper for Set 1, cf. Fig. 3(a) than for Set 3, cf. Fig. 3(b). This may be a consequence resulting from the dissimilarity in flow front shapes between the sets of experiments, since the capillary forces are acting perpendicular to the flow front.

This result indicates that the major mass transfer between regions with different scales takes place in the vicinity of the flow front, which is interesting for composite processing with particle doped resins where filtration may occur due to transport of fluid between the various scales. Adjustment of the injection velocity to avoid a non-homogeneous flow front may lead to a reduction in the particle filtration.

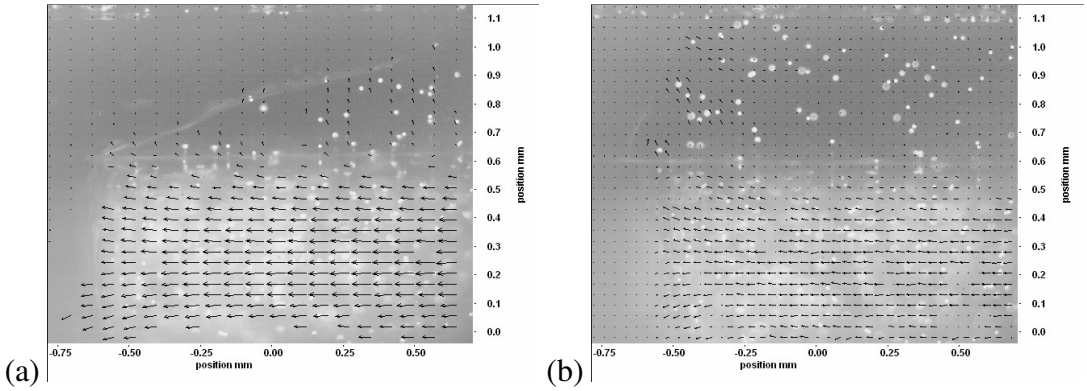

Fig. 3. Velocity field for (a) Exp 3 and (b) Exp 9 with 2x and 10x magnification, respectively.

In order to validate the experiments in the present work, comparison with theoretical velocity profiles for a steady state flow condition is performed. The steady state velocity profiles for the three sets of experiments show good agreement with the combined Stokes and Brinkman theoretical velocity profiles in the meso-scale channel and slit region, respectively, cf. Fig. 4(a). Fig. 4(b) shows a zoomed plot of the velocity profiles in the slit region together with the theoretical Brinkman velocity profiles, which strengthen the validity of the measurements of the flow field in the multi-scale channel.

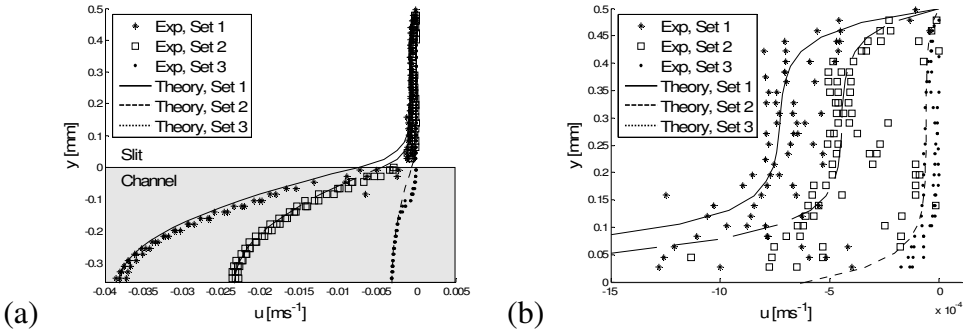

Fig. 4. Experimental and theoretical steady state velocity profiles in (a) half of the dual-scale channel and (b) the slit region.

Conclusions

In the present work an experimental study of the flow field in the vicinity of an advancing flow front in a dual-scale channel has been performed. It is shown that the region where the flow front is leading is shifted from the meso-scale channel region to the micro-scale slit region with decreasing injection velocity. It is also proved that the shape of the flow front in the dual-scale region varies significantly between the sets of experiments where higher injection velocity shows a lagging front in the slit region, whereas lower velocity indicates close to parallel fronts. It is also indicated that the penetration into the slit region is only acting in the very close vicinity of the parallel advancing fronts, whereas it acts over a larger area behind the front in flow conditions where the flow is clearly leading in the meso-scale channel region. The μPIV measurements are validated and show excellent agreement to theoretical steady state velocity profiles.

References

[1] Verrey, J., Michaud, V., and Månson, J.-A. E.: *Dynamic capillary effects in liquid composite moulding with non-crimp fabrics*. Composites: Part A, Vol. 37. 2006, No. 1, pp. 92-102.

[2] Pillai, K. M.: *Modeling the Unsaturated Flow in Liquid Composite Molding Processes: A Review and Some Thoughts*. Journal of Composite Materials, Vol. 38. 2004, No. 23, pp. 2097-2118.

[3] Patel, N., and James Lee, L.: *Effects of fiber mat architecture on void formation and removal in liquid composite molding*. Polymer Composites, Vol. 16. 1995, No. 5, pp. 386-399.

[4] Patel, N., and James Lee, L.: *Modeling of void formation and removal in liquid composite molding. Part I. Wettability analysis*. Polymer Composites, Vol. 17. 1996, No. 1, pp. 96-103.

[5] Patel, N., and James Lee, L.: *Modeling of void formation and removal in liquid composite molding. Part II. Model development and implementation*. Polymer Composites, Vol. 17. 1996, No. 1, pp. 104-114.

[6] Patel, N., Rohatgi, V., and Lee, L. J.: *Micro scale flow behaviour and void fromation mechanism during impregnation through a unidirectional stitched fiberglass mat.* Polymer Engineering Science, Vol. 35. 1995, No. 10, pp. 837-851.

[7] Binétruy, C., Hilaire, B., and Pabiot, J.: *The interactions between flows occurring inside and outside fabric tows during RTM*. Composite Science and Technology, Vol. 57. 1997, No. 5, pp. 587-596.

[8] Agelinchaab, M., Tachie, M. F., and Ruth, D. W.: *Velocity measurement of flow through a model three-dimensional porous medium*. Physics of Fluids, Vol. 18. 2006, No. 1, pp. 17105-1-11.

[9] Zhong, W. H., Currie, I. G., and James, D. F.: *Creeping flow through a model fibrous porous medium*. Experiments in Fluids, Vol. 40. 2006, No. 1, pp. 119-126.

[10] Shams, M., Currie, I. G., and James, D. F.: *The flow field near the edge of a model porous medium*. Experiments in Fluids, Vol. 35. 2003, No. 2, pp. 193-198.

[11] Tachie, M. F., James, D. F., and Currie, I. G.: *Velocity measurements of a shear flow penetrating a porous medium*. Journal of Fluid Mechanics, Vol. 493. 2003, No. 25, pp. 319-343.

[12] Goharzadeh, A., Khalili, A., and Jorgensen, B. B.: *Transition layer thickness at a fluid-porous interface*. Physics of Fluids, Vol. 17. 2005, No. 5, pp. 57102-1-10.

[13] Bown, M. R., MacInnes, J. M., and Allen, R. W. K.: *Micro-PIV simulation and measurement in complex microchannel geometries*. Measurement Science and Technology, Vol. 16. 2005, No. 3, pp. 619-626.

[14] Shavit, U., Bar-Yosef, G., and Rosenzweig, R.: *Modified Brinkman equation for a free flow problem at the interface of porous surfaces: The Cantor-Taylor brush configuration case*. Water Resources Research, Vol. 38. 2002, No. 12, pp. 561-5613.

[15] Buffone, C., Sefiane, K., and Christy, J. R. E.: *Experimental investigation of self-induced thermocapillary convection for an evaporating meniscus in capillary tubes using micro-particle image velocimetry*. Physics of Fluids, Vol. 17. 2005, No. 5, pp. 052104 -052104.

[16] Kyosuke, S., Yasuhiko, S., Arata, A., Akihide, H., Manabu, T., Takehiko, K., and Koji, O.: *High-speed micro-PIV measurements of transient flow in microfluidic devices*. Measurement Science and Technology, Vol. 15. 2004, No. 10, pp. 1965.

[17] Brinkman, H. C.: *On the permeability of media consisting of closely packed porous particles*. Applied Science Research, Section A, Vol. 1. 1947, No. 81.

[18] Batchelor, G. K.: *An introduction to fluid mechanics*, Cambridge University Press. London, 2000.

[19] Wereley, S. T., and Meinhart, C. D.: *Second-order accurate particle image velocimetry*. Experiments in Fluids, Vol. 31. 2001, No. 3, pp. 258-268.

[20] Meinhart, C. D., Wereley, S. T., and Santiago, J. G.: *A PIV algorithm for estimating time-averaged velocity fields*. Journal of Fluids Engineering, Vol. 122. 2000, No. 2, pp. 285-289.

[21] Forsythe, W. E.: *Smithsonian physical tables*, Knovel. Norwich, N.Y., 2003.

Authors

MSc. Nordlund, Markus
Dr. Lundström, T. Staffan
Division of Fluid Mechanics
Department of Applied Physics and Mechanical Engineering
Luleå University of Technology
SE-97187 Luleå, Sweden
E-mail: Markus.Nordlund@ltu.se